Investigation of the structural and electrical properties of Al-Ni the ferrite and effect of Yttrium

AbdHakeem A. AbdAlgaleel Al-Hammadi
Physics Department, Faculty of Science, Sana'a University, Sana'a, Yemen
DOI: https://doi.org/10.47372/uajnas.2015.n1.a18

Abstract

The aim of the present work is to prepare some samples of the S-type spinel ferrite $Al_{0.51-0.51x}Ni_xFe_{2.16-0.16x}O_4$ and $Al_{0.51-0.51x}Ni_xFe_{2.06-0.16x}Y_{0.1}O_4$ where (x = 0.0, 0.5, and 1) to investigate some of their structure and different electric properties as a function of temperature, frequency and compositions. The X-ray diffraction analysis of the samples ensures the formation of S-type spinel ferrite with the average particle size estimated as 35.1-35.9nm. Ac conductivity, dielectric constant and loss tangent were investigated by using the complex impedance technique. The conductance results specified two types of conduction mechanisms, hopping conduction and displacement conduction of charge carriers quantum-mechanical-tunneling, QMT and correlated barrier hopping, CBH in the studied range of temperature. Cole-Cole diagrams show as expected the existence of a distribution of relaxation times and gave values of the activation energy of the dielectric relaxation process ranging from -0.022eV to 0.173eV.

Key words: Al-Ni-Fe-Y Oxides; Nano crystal; Electrical conductivity; Dielectric properties**.**

Introduction

Ferrites are iron containing complex oxides with often interesting electrical and magnetic properties. Nowadays, they play an important role in the field of electronics industry because they are relatively inexpensive, more stable and easily manufactured [11,12].

Ferrites are used in applications from simple lifting magnets to the most complex microwave communications to outer space. In many cases, there are no practical alternative materials. Even the guidance system that is used by birds and other animals to return home after migration has been postulated to involve ferrites similar to man-made mechanical counterparts [11].

Ferrites are also widely used in microwave devices, permanent magnets, high-density magnetic and magneto-optic recording media. The whole field of high frequency telecommunications in the frequency range from 10^3 to 10^{11} Hz would look very different, but for the many useful properties of ferrites; spinel, garnets and hexagonal compounds are alike. For each particular application, many material parameters play a role. A distinction can be made between intrinsic parameters and those that are related to the nanostructure. The intrinsic parameters depend on the crystal structure of the lattice [11,12].

The study of the complex dielectric constant of the transition metal oxides, particularly spinel ferrites, is of great importance from both the fundamental and the applied research points of view [11,17]. These properties are quite sensitive to the preparation conditions, in addition to the amount and type of substitution [21]. A^{3+} -ferrite is an important material for applications at microwave frequencies; especially as isolators, circulators, gyrators etc. [19]. The modification in electric and magnetic properties of A^{3+}-ferrites, by substitution of different ions, has been studied by many investigators, [17,21,19,26,25,22,1,2]. In the present investigation a systematic study of the complex dielectric constant and loss tangent tanδ of Yttrium - Al-Ni ferrites has been carried out and the results are given in this paper.

Experimental Method

High purity oxides of Fe_2O_3, NiO , Al_2O_3 and Y_2O_3 oxides were mixed together in molar ratio to prepare mixed ferrites with the composition S-type spinel ferrite to investigate some of their structure and some of their different electric properties as: $Al_{0.51-0.51x}\,Ni_x\,Fe_{2.16-0.16x}\,O_4$ and $Al_{0.51-0.51x}$

$Ni_x\ Fe_{2.06-0.16x}\ Y_{0.1}\ O_4$ where (x = 0.0, 0.5, and 1). The oxides corresponding were thoroughly mixed in and were ground to fine powders using a gate mortar for 1h for each sample, and then each sample was ground again for 3hs using a mechanical grinding machine. The final product was pre-sintered in air at 1170K for 6hs and then slowly cooled to room temperature. The pre-sintered mixture was ground and fired again at 1270K for 6h in order to improve homogeneity of the samples. The mixture was ground again for 3hs for each sample, using the mechanical grinding machine, to prepare very fine powder. Pellets were prepared by pressing the final product under constant pressure 29.4 x 10^7 N/m^2 into discs. The discs were finally sintered at 1470K for 6hs and then slowly cooled to room temperature by turning off the furnace. Finally, the surfaces of the disc were polished and coated with silver paste as a contact material for electrical measurements.

The dielectric constant was measured under vacuum at different temperatures and different frequencies by using the complex impedance measuring technique (Lock-in amplifier Stanford SR 510 type, U.S.A.) which measures the frequency, phase angle and voltage drop developed across a standard resistor connected in series with the sample.

Results and Discussions

X- ray, lattice parameter a and crystallite size

The interplanar distance, d, Miller indices (hkl), and relative intensities, I/I_o, (where I_o is the maximum intensity) were recorded for each pattern. The samples were compared with the results of JCPDS card (Joint Committee on Powder Diffraction Standard) for $NiFe_2O_4$, $NiAl_2O_4$ and $FeAl_2O_4$ with single phase cubic spinel ferrite[15]. Table (1) shows the X-ray results of the samples in comparison with the results of JCPDS card.

Table (1). d-spacing and relative intensities of $Al_{0.51-0.51x}Ni_xFe_{2.16-0.16x}O_4$ and $Al_{0.51-0.51x}Ni_xFe_{2.06-0.16x}\ Y_{0.1}O_4$ where (x = 0.0, 0.5, and 1) and those obtained by JCPDS cards

	JCPDS card Al_2FeO_4		The prepared samples												JCPDS card $NiFe_2O_4$	
			$Al_{0.51}Fe_{2.16}O_4$		$Al_{0.51}Y_{0.1}Fe_{2.06}O_4$		$Al_{0.255}Ni_{0.5}Fe_{2.08}O_4$		$Al_{0.255}Ni_{0.5}Fe_{1.98}Y_{0.1}O_4$		$Ni_{0.5}Fe_{1.9}Y_{0.1}O_4$		$NiFe_2O_4$			
hkl	d_{hkl}	I/I_o	d_{hkl}	I/I_o	d_{hkl}	I/I_o	d_{hkl}	I/I_o	d_{hkl}	I/I_o	d_{hkl}	I/I_o	d_{hkl}	I/I_o	d_{hkl}	I/I_o
111	4.709	3	4.738	9	---	---	4.782	11	---	---	4.839	19	4.837	18	4.82	20
220	2.883	58	2.853	34	2.963	35	2.913	35	2.979	31	2.962	37	2.954	33	2.948	30
311	2.459	100	2.421	100	2.539	100	2.485	100	2.534	100	2.525	100	2.514	100	2.513	100
222	--	---	2.313	3	---	---	2.313	4	---	---	2.418	8	2.415	7	2.404	8
400	2.038	17	2.086	39	2.096	19	2.088	22	2.094	22	2.095	22	2.091	21	2.085	25
422	1.665	16	1.645	13	1.704	8	1.686	9	1.713	12	1.713	11	1.701	8	1.702	8
511	1.569	36	1.536	21	1.607	23	1.588	24	1.612	23	1.615	21	1.605	21	1.605	30
440	1.441	42	1.475	24	1.477	28	1.476	30	1.480	29	1.481	32	1.465	27	1.476	40
620	1.289	5	1.29	17	----	---	1.301	5	---	---	1.324	5	1.315	4	1.318	6
533	1.243	8	1.275	9	1.277	7	1.278	7	1.289	7	1.289	7	1.279	7	1.271	10

The lattice parameter, a, was calculated using the following relation;

$$a = d_{hkl}\sqrt{h^2 + k^2 + l^2}$$

The values of $(h^2+k^2+l^2)$ were plotted versus $1/d^2$ for all the samples. The values of lattice constant, a, for each composition were calculated from the slopes of the lines. The value of the lattice constant for $NiFe_2O_4$ is 0.8344nm and for $Al_{0.51}Fe_{2.16}O_4$ is 0.8149nm. These values are in agreement with that obtained by JCPDS card, where for $NiFe_2O_4$, the lattice constant is 0.8339nm, and for Al_2FeO_4, a = 0.81534nm

For the Yttrium substitute composition the lattice parameter of the samples for $Al_{0.51}\ Fe_{2.06}\ Y_{0.1}\ O_4$ is 0.818nm and for $Ni\ Fe_{2.06}\ Y_{0.1}\ O_4$ is 0.8381nm.

The lattice parameter increases slightly by increasing Ni-content. This behavior may be attributed to ionic radii of the ingredient ions. r_{Ni} is the radius of Ni^{2+} ion (= 0.069nm [12]), r_{Fe} is the ionic radius of Fe^{3+} ion (=0.064nm [12]), r_{Al} is the ionic radius of Al^{3+} ion (= 0.055nm [12]) and r_y is the ionic radius of Y^{3+} ion (= 0.091nm [12]).

The mean crystallite size may be estimated from the half width value of the XRD peak (311), using the Scherrer's equation[13,9], $D = \frac{k_s \lambda}{\beta \cos\theta}$

Where λ is the x-ray wave length, β the width of a strong peak in radians at half maximum intensity, θ the corresponding Bragg angle and k_s is the Scherrer's constant which has a value of 0.95 or 0.94 [13,9]. Table (2) shows the grain size D of the samples.

Table (2). The value of the grain size with Ni-ion content

X (Nickel content)	Grain size (D) (nm) at room temperature	Grain size (D) with Yttrium (nm) at room temperature
1	35.874	35.886
0.5	35.895	35.197
0	35.904	35.197

Complex dielectric and conductivity behavior

Figure(1) represents the Logarithmic scale of dielectric constant and conductivity of the sample with x=0, the higher temperature T=293K and the frequency range 170Hz to10^5Hz,. The figure also shows the real and imaginary parts of dielectric and conductivity as a function of frequency. The two parts of dielectric σ` and σ`` are in the first quadratic with positive value, while the two parts of conductivity σ` and σ``, are in the fourth quadratic with negative value. The ε`` decreases by increasing frequencies at room temperature. The ε` decreases with the increase of frequency until 3162Hz and begins to increase with a small period of increasing frequency. After that, remains constant with increasing frequency.

The conductivity σ`` increases in negative direction with the increase of frequencies, at room temperature, until 3162Hz and begins to decrease by increasing the frequency. The σ` appears a constant behavior by increasing the frequency. (percentage error in this sample is 0.015% -0.013%).

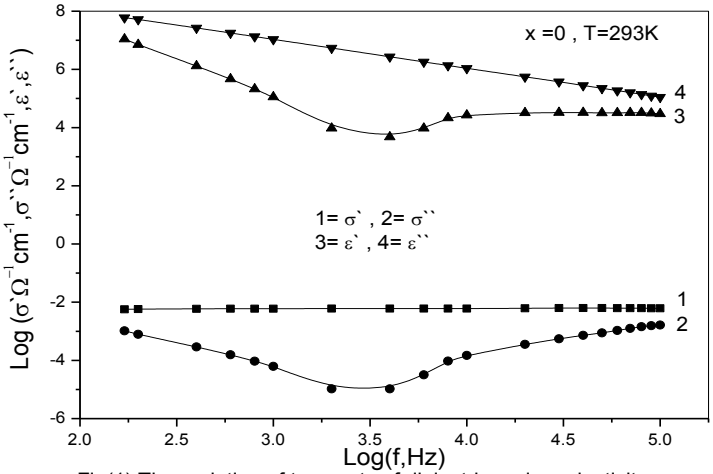

Fig(1).The variation of two parts of dielectric and conductivity with frequency for $Al_{0.51}Fe_{2.16}O_4$ at room temperature (T=293K).

Figures(2,3,4) represent the sample with x=0 and Yttrium, the range of temperature 299K, room temperature to 560k and the same frequency range.

In the range of temperatures 299K-367K, the two parts of dielectric ε' and ε'' give a constant value by increasing the frequency, that except The ε'' appears as little decreasing at high frequency between 8×10^4Hz and 10^5Hz. The two parts of conductivity σ` and σ`` decrease with the increasing of frequency, except σ` that appears as little increasing between 8×10^4Hz and 10^5Hz. (percentage error for all other samples is less than < 0.01%).

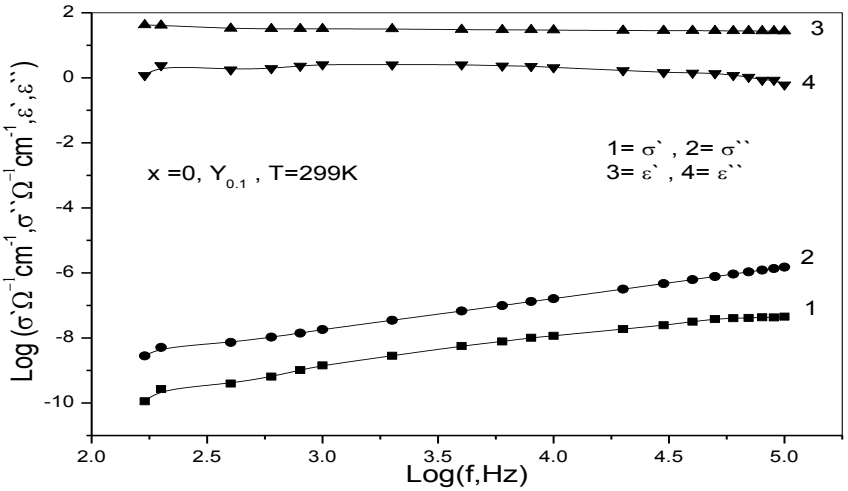

Fig(2).The variation of two parts of dielectric and conductivity with frequency for $Al_{0.51}Fe_{2.06}Y_{0.1}O_4$ at range of temperature T=299K.

The same Figures (3,4) with temperatures from 406K to 483K show three behavior of dielectric and conductivity with frequency. The figures also show the intersection between the two parts of dielectric ε`, ε`` and the two parts of conductivity σ`, σ``. The point of intersection shifts to the direction of a higher frequency with the increasing temperature and divide the dielectric and conductivity into eight parts. The behavior of dielectric and conductivity below intersection point shows ε`` > ε` and σ` > σ`` and, above this point, shows ε` > ε`` and σ`` > σ`.

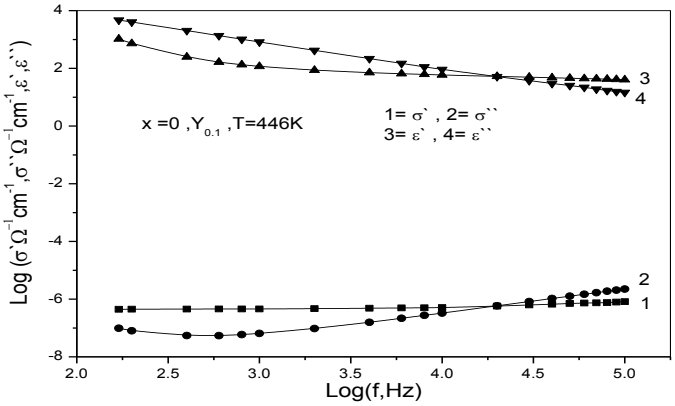

Fig(3).The variation of two parts of dielectric and conductivity with frequency for $Al_{0.51}Fe_{2.06}Y_{0.1}O_4$ at range of temperature T=446K.

Figures(4) show the dielectric and conductivity as a function of frequency. The behavior of the two parts of dielectric and conductivity in the temperature range 505k -560K show the same behavior of the sample with x=0 Figure (1)

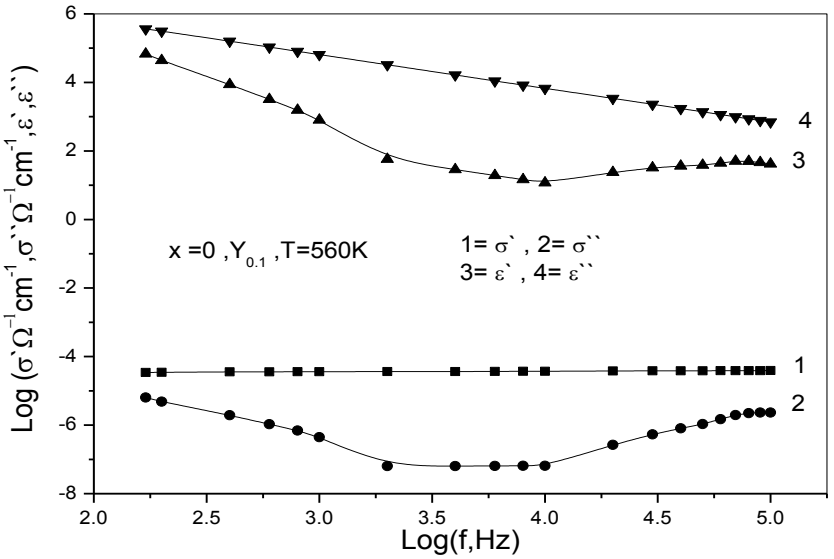

Fig(4).The variation of two parts of dielectric and conductivity with frequency for $Al_{0.51}Fe_{2.06}Y_{0.1}O_4$ at range of temperature T=560K.

Figures (5,6) show the real and imaginary parts of conductivity and dielectric versus frequency in the logarithmic scale for the sample with x=0.5 and 0.1 yttrium. The real and imaginary parts of conductivity σ' and σ'' slightly decreases with increasing frequencies at room temperature. When the temperature increase above room temperature, the imaginary parts □'' increase by increasing the frequency at low frequency, and this period of increasing in the conductivity σ'' shift to higher frequency by increasing the temperature. That's mean the maximum points of σ'' in the negative direction shifts to higher frequencies as the temperatures increases.

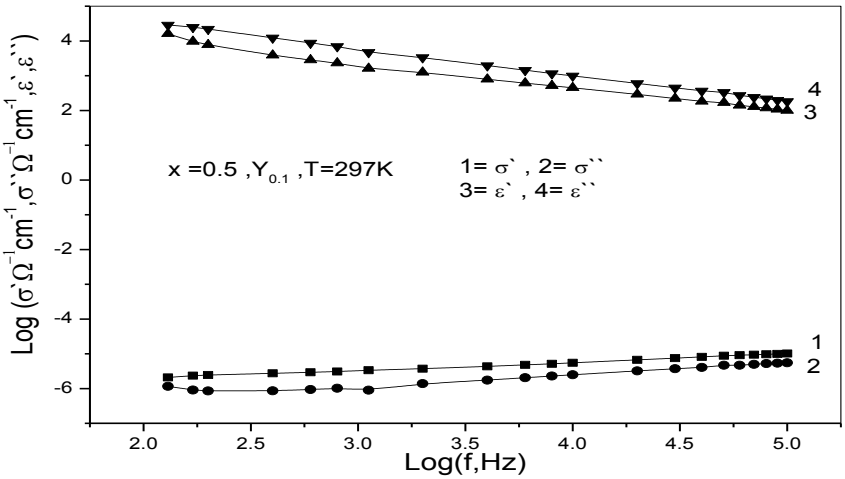

Fig(5).The variation of two parts of dielectric and conductivity with frequency for $Al_{0.255}Ni_{0.5}Fe_{1.98}Y_{0.1}O_4$ (T=297K).

Figures (6) show the same behavior of the sample with x=0 Figure(1) and Figure(4)

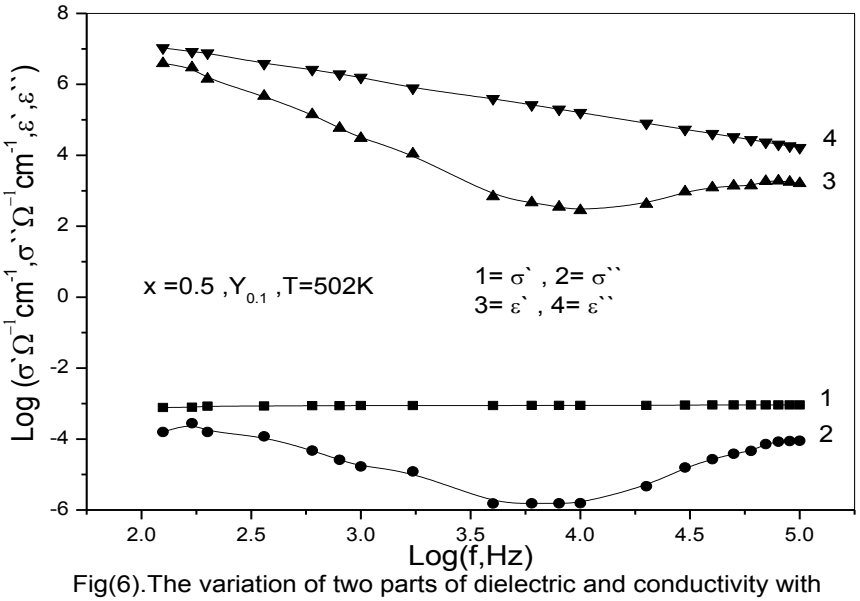

Fig(6).The variation of two parts of dielectric and conductivity with frequency for $Al_{0.255}Ni_{0.5}Fe_{1.98}Y_{0.1}O_4$ (T=502K).

Figures (7,8) represent the behavior of dielectric and conductivity with frequency at temperature T=333K for the sample with x=1,. The dielectric and conductivity show the intersection between the two parts of dielectric ε`, ε`` and the two parts of conductivity σ`, σ``. The point of intersection shifts to the direction of a higher frequency with the increasing of temperature (T=299k to 383K) and divide the dielectric and conductivity into eight parts, inside and outside. The behavior of dielectric and conductivity below intersection point shows ε`` > ε` and σ`` > σ` and, above this point shows ε` > ε`` and σ` > σ``.

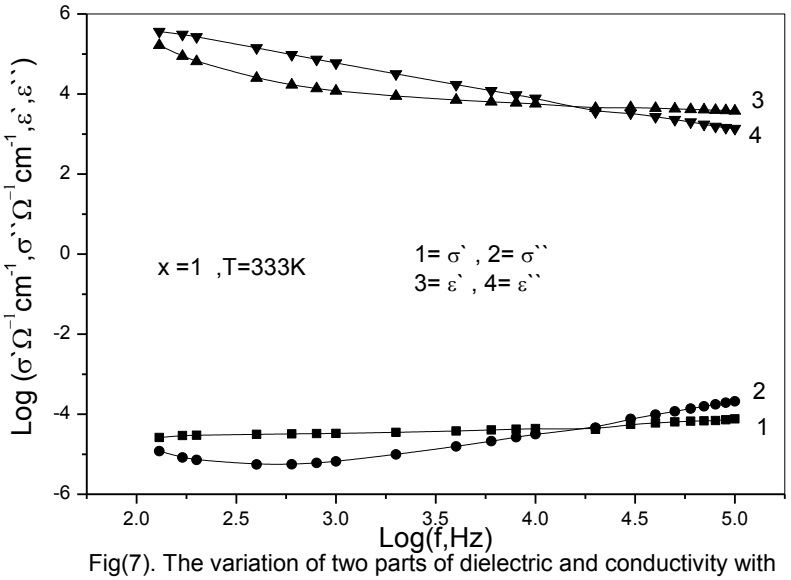

Fig(7). The variation of two parts of dielectric and conductivity with frequency for $Ni\ Fe_2O_4$ at temperature T=333K.

Figures (8) represent the sample with x=1, the range of temperature is 393K to 428K, the same frequency range. The two parts of conductivity σ' and σ'' give a constant value with the increasing of frequency, except σ'' that appears with a little decreasing at high frequency between 8×10^4Hz and 10^5Hz.. The two parts of dielectric ε` and ε`` decrease with the increase of frequency, except ε` that appears with a little increasing between 8×10^4Hz and 10^5Hz.

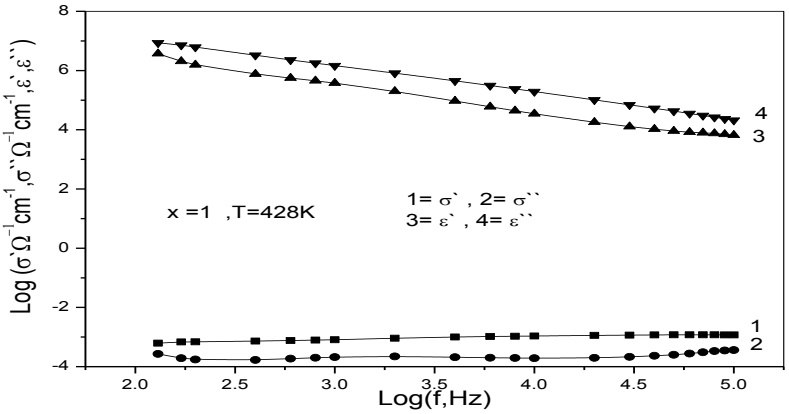

Fig(8). The variation of two parts of dielectric and conductivity with frequency for Ni Fe_2O_4 at range of temperature T=428K.

Figures(9,10) represent the behavior of dielectric and conductivity with frequency for the sample with x=1, and 0.1 yttrium. The dielectric and conductivity show the intersection between the two parts of dielectric ε`, ε`` and the two parts of conductivity σ`, σ``. The point of intersection shifts to the direction of a higher frequency with the increase of temperature (T=293k to 359K) and divide the dielectric and conductivity, into eight parts.

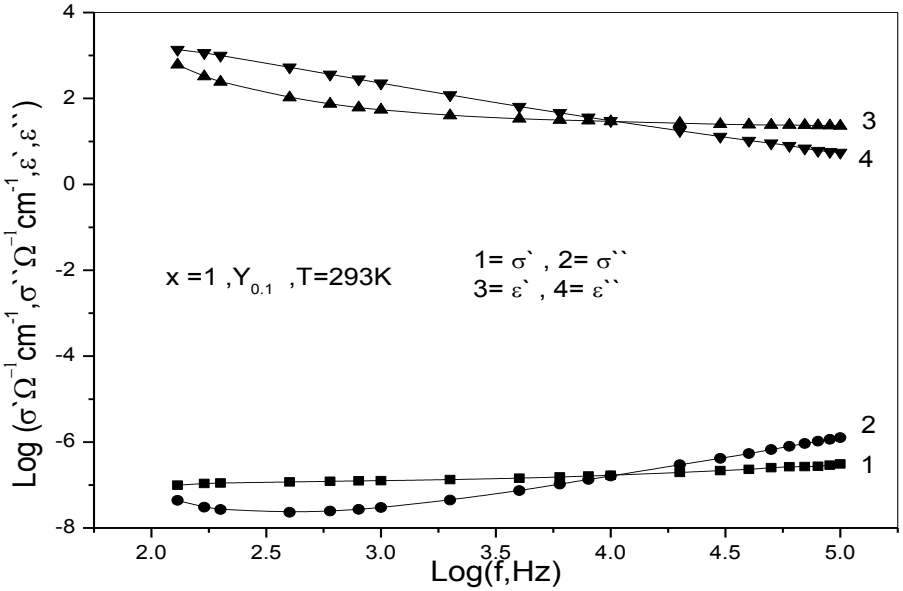

Fig(9).The variation of two parts of dielectric and conductivity with frequency for Ni $Fe_{1.9}$ $Y_{0.1}$ O_4 at temperature (T=293K).

The behavior of dielectric and conductivity, below intersection point, it shows ε`` > ε` (where ε`` decrease linearly with frequency, ε` show a curve decreasing with frequency) and σ`` > σ` (where σ`` show a curve increase and decrease with frequency, σ` is a constant with frequency) and above this point shows ε` > ε`` (where ε` is a constant and ε`` decrease with frequency) and σ` > σ`` (.where σ`` decrease and σ` is constant with frequency).

At high temperature, T=367k to 403K, the behavior of the two parts of dielectric and conductivity shows the same behavior of the sample with x=0.

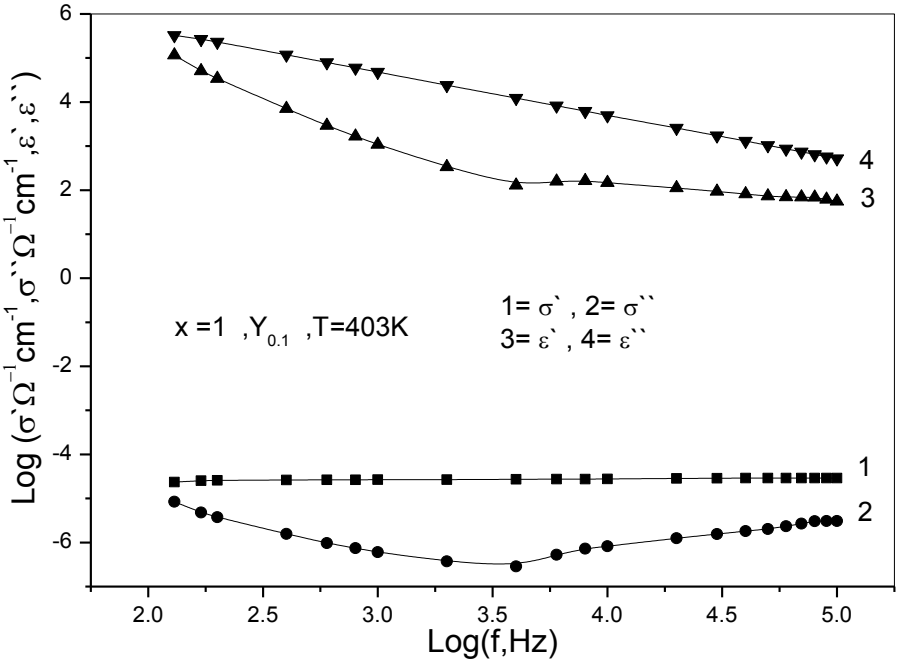

Fig(10).The variation of two parts of dielectric and conductivity with frequency for Ni $Fe_{1.9}$ $Y_{0.1}$ O_4 at temperature (T=403K).

Figures (11) to Figures(16) show the variation of the imaginary part of dielectric constant ε'' as a function of the real part of dielectric ε', with frequency range 200Hz-100KHz and selected temperatures for the substituted composition $Al_{0.51-0.51x}$ Ni_x $Fe_{2.16-0.16x}$ O_4 and $Al_{0.51-0.51x}$ Ni_x $Fe_{2.06-0.16x}$ $Y_{0.1}$ O_4 where (x = 0.0, 0.5, and 1). The result of the two parts of dielectric ε = ε' + Jε'' shows semicircle curve. The two parts of dielectric show a dispersion at a high value of dielectric with low frequency and correlation at low value of dielectric with high frequency. The dielectric ε locus is a semicircle in the first quadrant of ε, as shown in the figures.

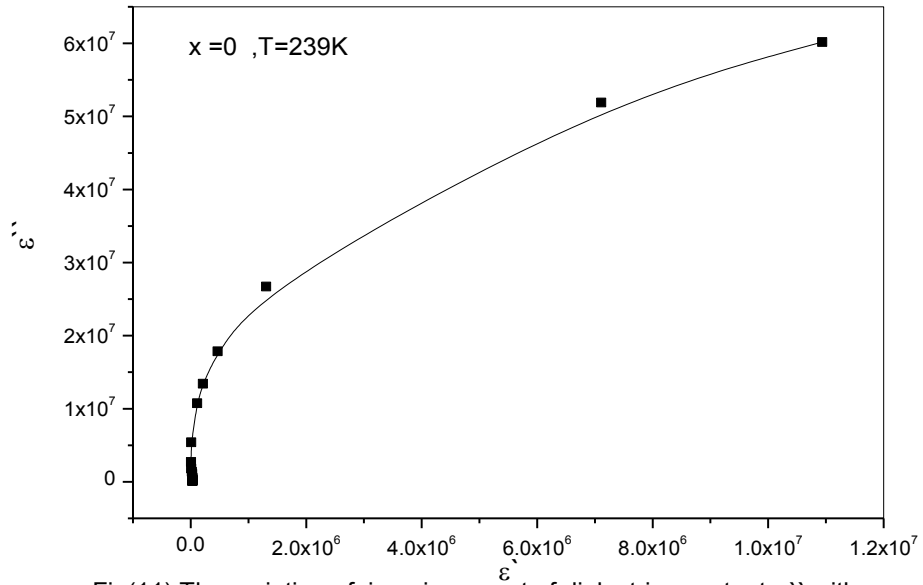

Fig(11).The variation of imaginary part of dielectric constant ε`` with real part ε` for $Al_{0.51}Fe_{2.16}O_4$ at room temperature (T=293K).

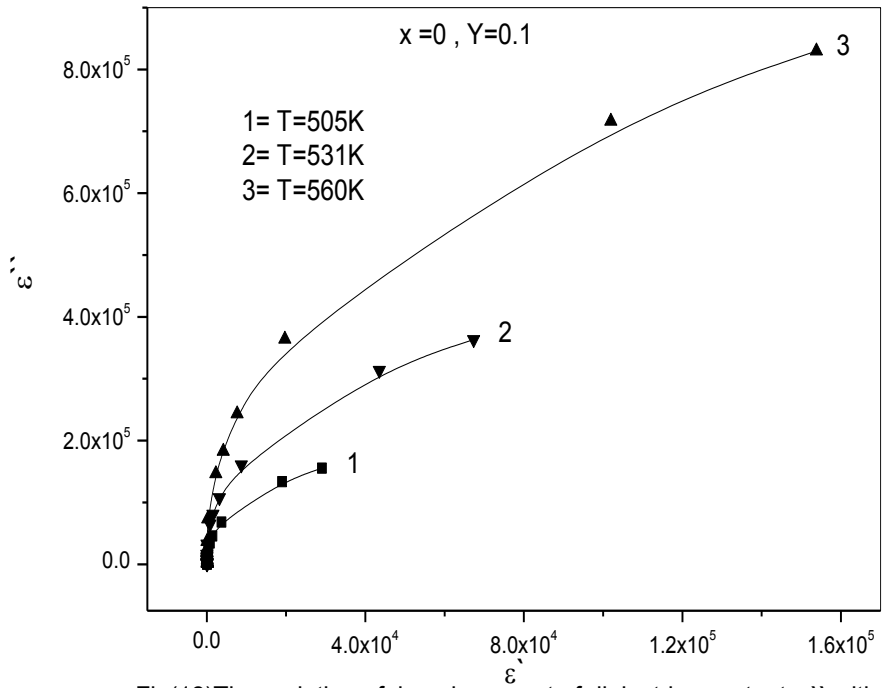

Fig(12)The variation of imaginary part of dielectric constant ε`` with real part ε` for $Al_{0.51}Fe_{2.06}Y_{0.1}O_4$ (T=505K-560K)

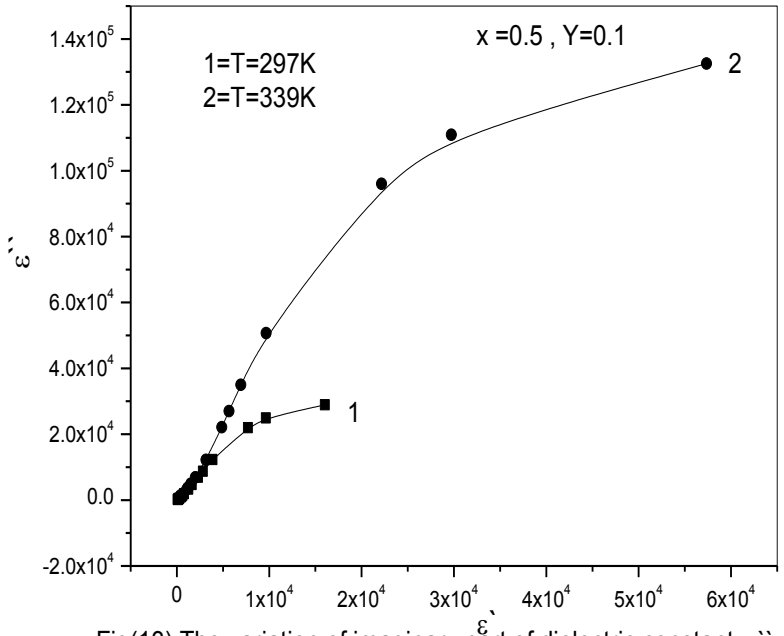

Fig(13).The variation of imaginary part of dielectric constant ε`` with real part ε` for $Al_{0.255}$ $Ni_{0.5}$ $Fe_{1.98}$ $Y_{0.1}$ O_4 (T=297K -339K).

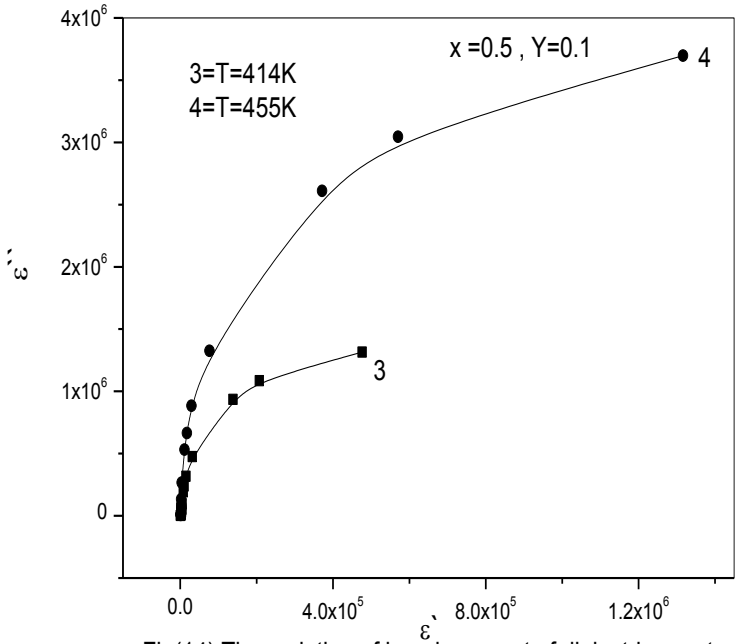

Fig(14).The variation of imaginary part of dielectric constant ε`` with real part ε` for $Al_{0.255}$ $Ni_{0.5}$ $Fe_{1.98}$ $Y_{0.1}$ O_4 (T=414K -455K).

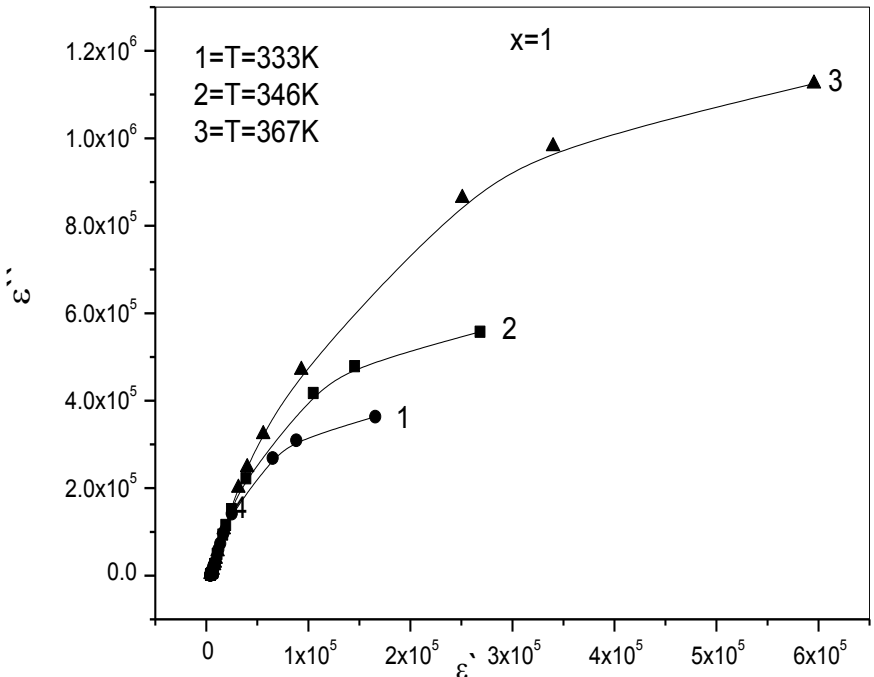

Fig(15)The variation of imaginary part of dielectric constant ε`` with real part ε` for Ni Fe_2 O_4 at range of temperature T=333K-367K.

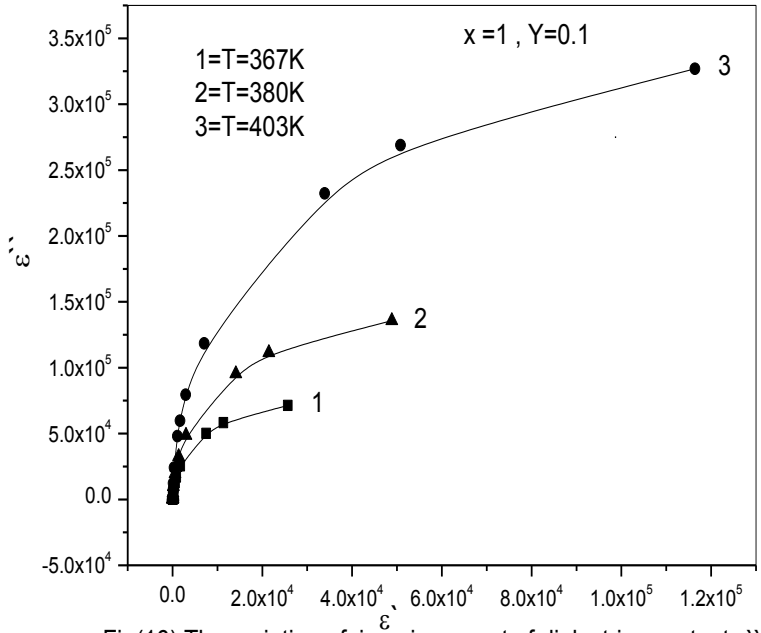

Fig(16).The variation of imaginary part of dielectric constant ε`` with real part ε` for Ni $Fe_{1.9}$ $Y_{0.1}$ O_4 at temperature (T=367K-403K).

Figure(17) to Figures(24,25) show the variation of the real part of conductivity σ' as a function of the imaginary part of conductivity σ'', with frequency range 170Hz-100KHz and selected temperatures. The result of the two parts of conductivity σ= σ' + Jσ`` shows a three lines or two curves at a high value of the two parts of conductivity and two lines or one curve at low value of two parts of conductivity, however the relation between the two parts of conductivity show the curve in the mid region. The conductivity shows a dispersion at high and low values of the two parts of conductivity and a correlation in mid region as a line or curve at each temperature This behavior appears for the sample with x=0 (Aluminums and irons) at 293K and x=0 with 0.1 yttrium (Aluminums, irons and yttrium) at T= 528K. The behavior of the two parts of conductivity of the same sample with 0.1 yttrium at 560k (also for other samples at high temperature) shows a correlation on mid region and upper region. The conductivity at room temperature and above room show dispersion at high value and correlation at low value of parts of conductivity for the samples at each temperature. The conductivity σ locus is a lines or curve with three phases in the third quadrant of σ, as shown in the figures.

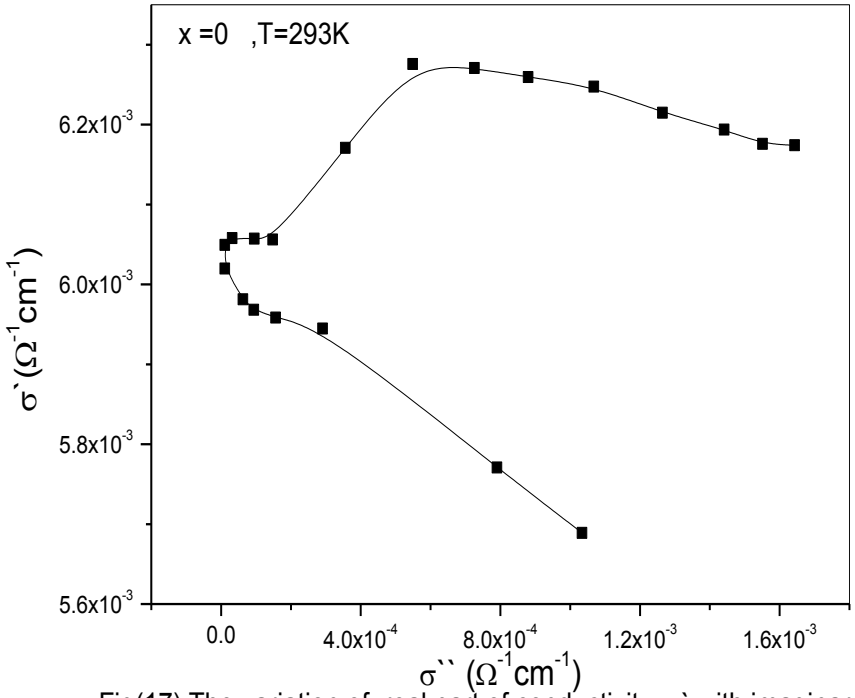

Fig(17).The variation of real part of conductivity σ` with imaginary part σ`` for $Al_{0.51}Fe_{2.16}O_4$ at room temperature (T=293K).

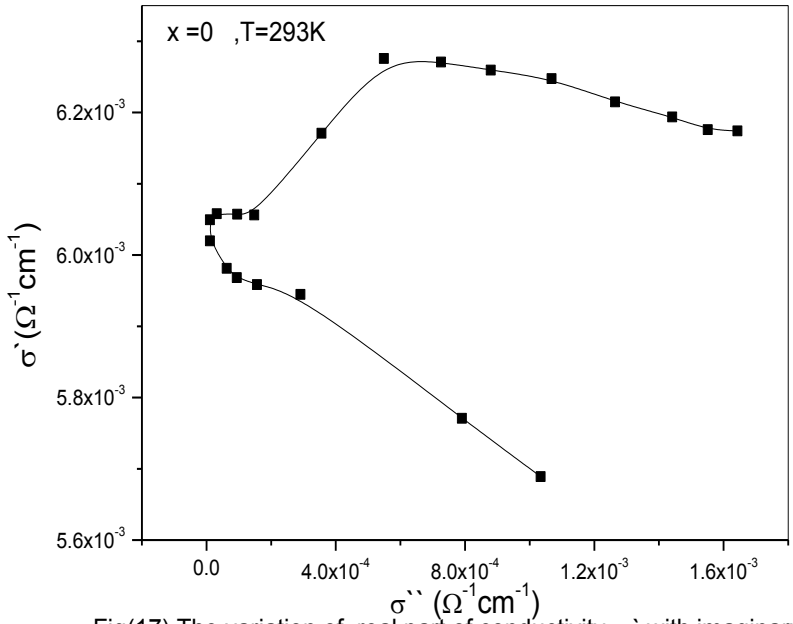

Fig(17).The variation of real part of conductivity σ` with imaginary part σ`` for $Al_{0.51}Fe_{2.16}O_4$ at room temperature (T=293K).

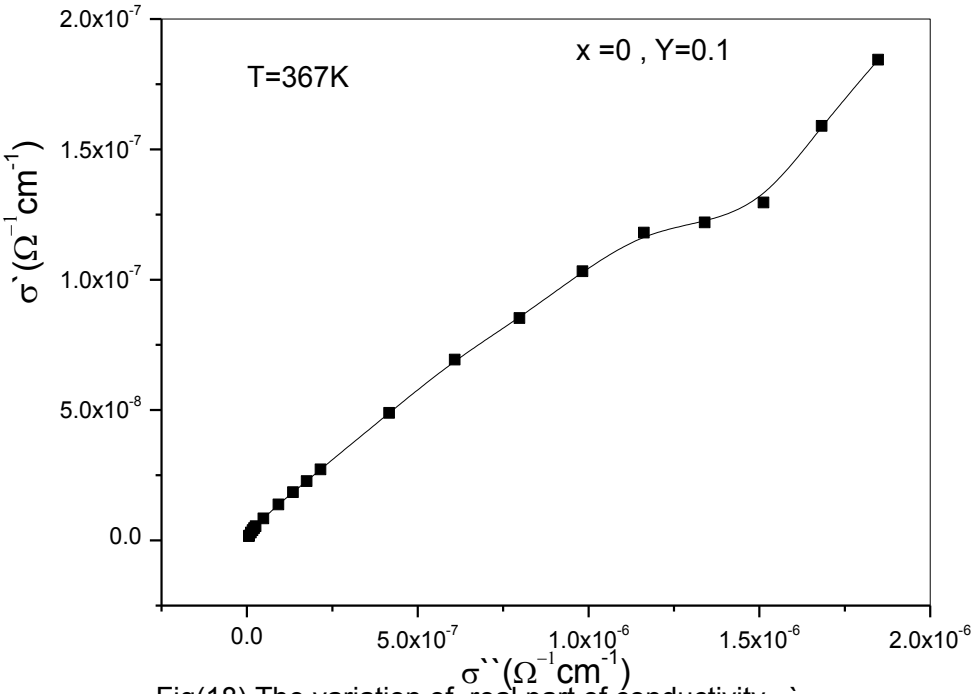

Fig(18).The variation of real part of conductivity σ` with imaginary part σ`` for $Al_{0.51}Fe_{2.06}Y_{0.1}O_4$ (T=367K).

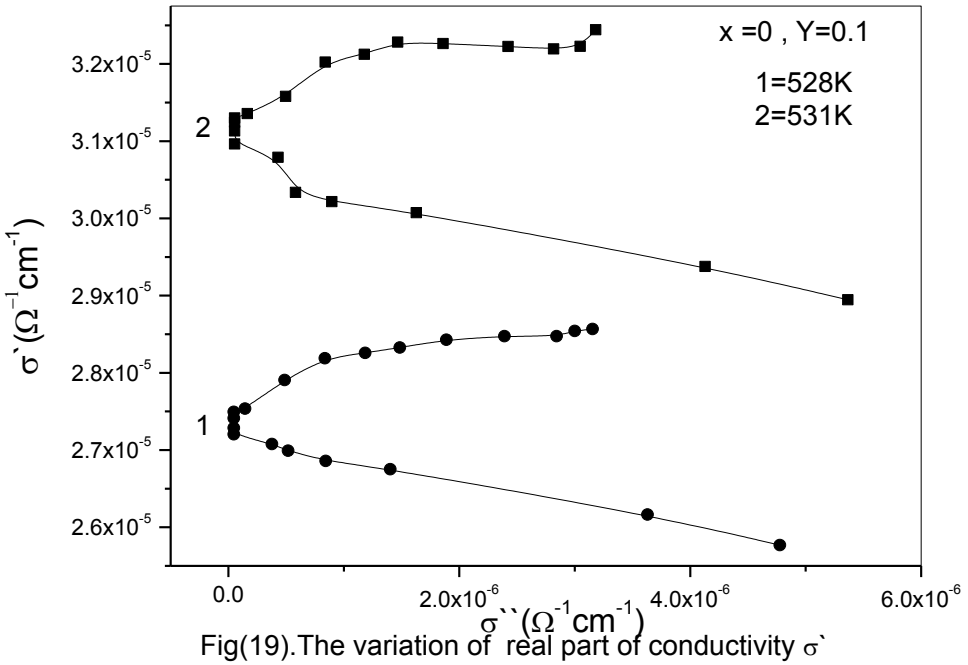

Fig(19).The variation of real part of conductivity σ` with imaginary part σ`` for $Al_{0.51}Fe_{2.06}Y_{0.1}O_4$ (T=528k-531K).

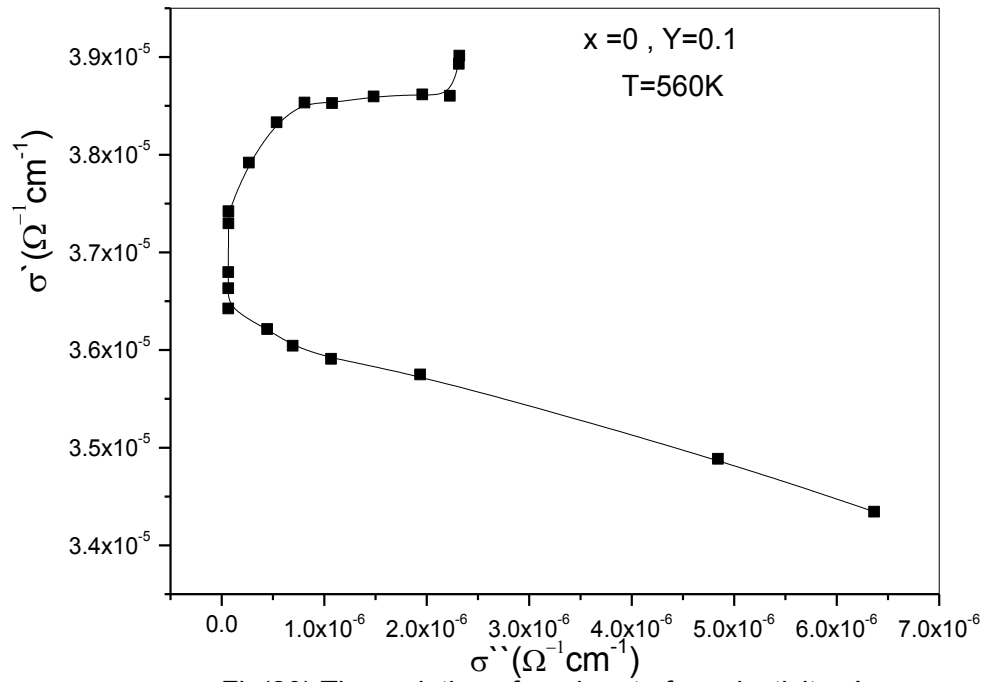

Fig(20).The variation of real part of conductivity σ` with imaginary part σ`` for $Al_{0.51}Fe_{2.06}Y_{0.1}O_4$ (T=560K).

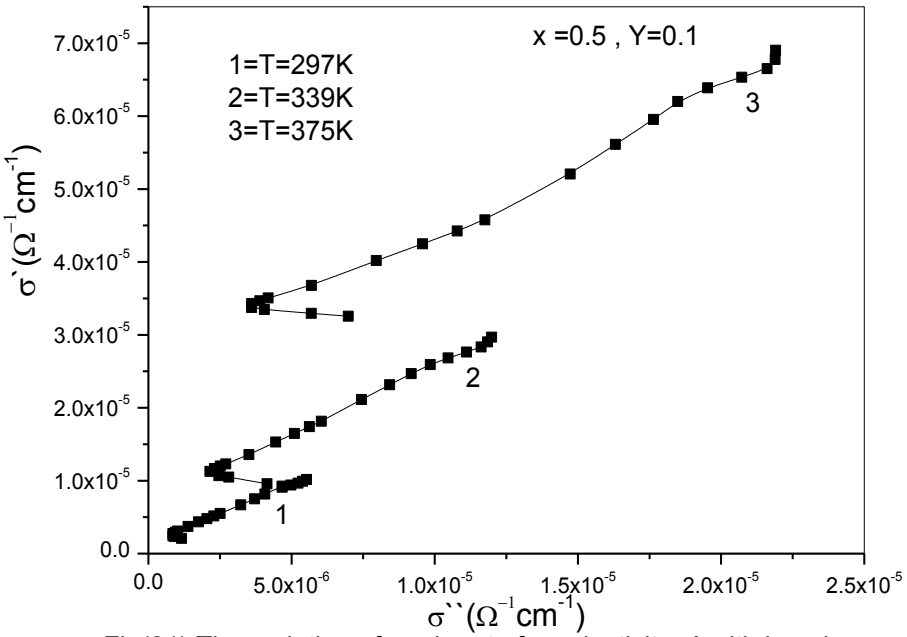

Fig(21).The variation of real part of conductivity σ` with imaginary part σ`` for $Al_{0.255}Ni_{0.5}Fe_{1.98}Y_{0.1}O_4$ (T=297K -375K).

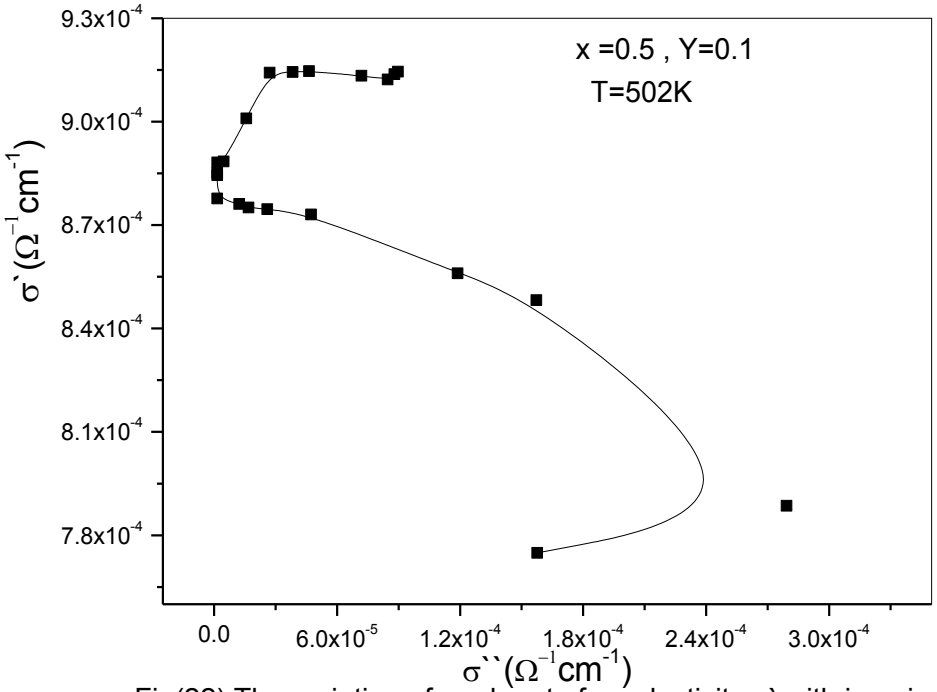

Fig(22).The variation of real part of conductivity σ` with imaginary part σ`` for $Al_{0.255}Ni_{0.5}Fe_{1.98}Y_{0.1}O_4$ (T=502K).

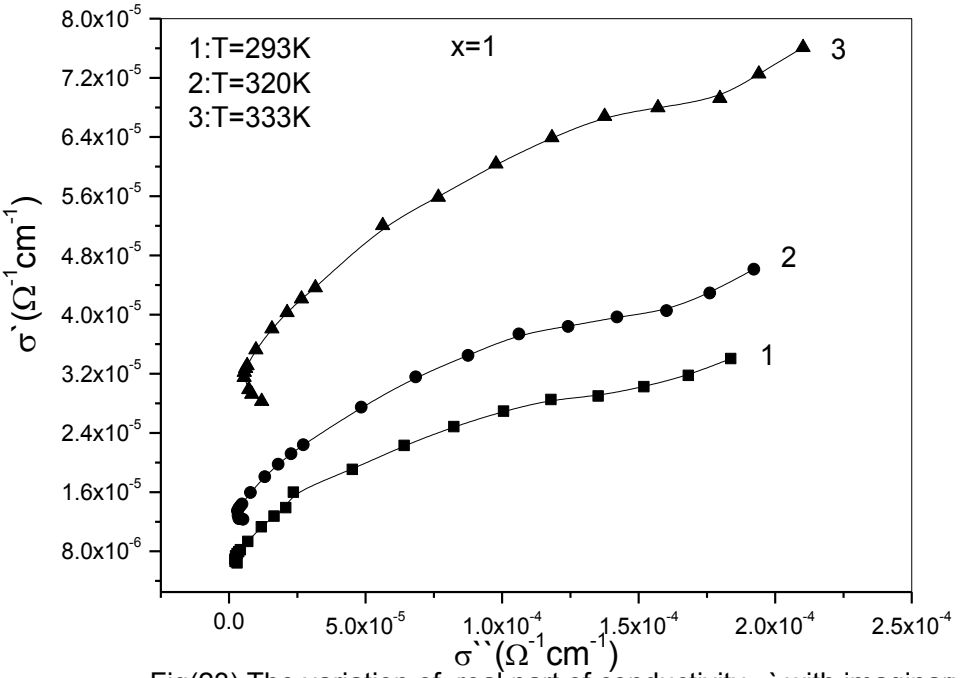

Fig(23).The variation of real part of conductivity σ` with imaginary part σ`` for Ni Fe_2O_4 at range of temperature T=293K-333K.

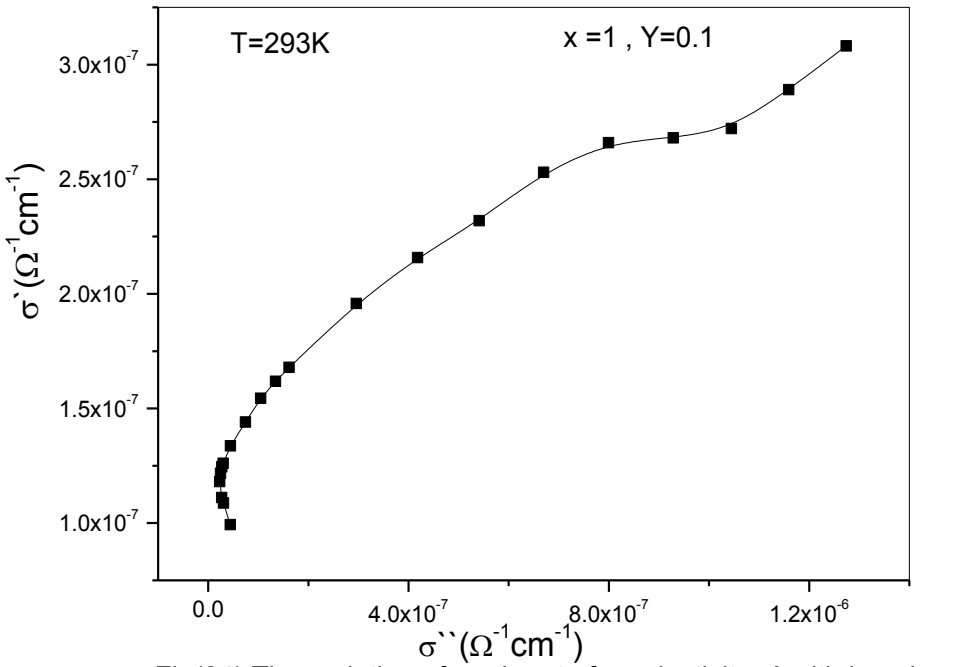

Fig(24).The variation of real part of conductivity σ` with imaginary part σ`` for Ni $Fe_{1.9}Y_{0.1}O_4$ at temperature (T=293K).

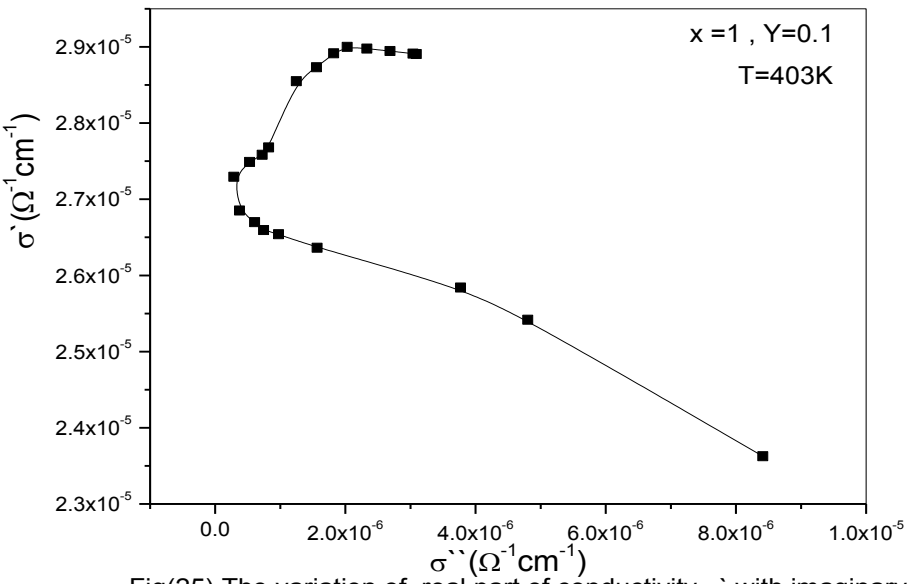

Fig(25).The variation of real part of conductivity σ` with imaginary part σ`` for Ni $Fe_{1.9}Y_{0.1}O_4$ at temperature (T=403K).

The relative positions and the distance of σ and ε from the respective origins are different, while the angles with the horizontal axis are equal, but of opposite sign.

Generally, at low frequencies and low temperature (T=293k, room temperature) the value of the tow parts of dielectric constant is high and decreases with the increase of frequency. The high value of ε' and ε'`, at low frequency, can be explained on the basis of Maxwell Wagner two layer model and Koop`s phenomenological theory [18]. According to this model, ferrite samples, with inhomogeneous structure, can be considered to consist well conducting grains having parameters σ_1, ε_1, d_1 separated by highly resistive thin layers having parameters σ_2, ε_2, d_2 where d_1 and d_2 are the thickness of grain and grain boundary, respectively. So, the low frequency dielectric constant of the samples can be written as

$$\varepsilon' = \varepsilon_2 / x, \quad \text{where} \quad x = d_1/d_2 \qquad (1)$$

$$\varepsilon'' = \varepsilon_1 / x, \quad \text{where} \quad x = d_1/d_2 \qquad (2)$$

This explains the high values of the low frequency of the two parts of dielectric constant [3,23,4]. Normally, the impedance and admittance spectrum of a polycrystalline material is expected to have three semicircular arcs: one attributed to the grain, the second to the grain boundary, and the third semicircle corresponds to the space charge polarization. However, the samples under investigation show the third depressed semicircle arcs, as shown in the figures of complex conductivity, especially at high temperatures for each samples. The relations between the impedance, Z, and the admittance, Y, and the complex admittance is given as:

$$Z = 1/Y . \qquad (3)$$

The experimental data obtained is often performed and analyzed in terms of complex conductivity with real part σ`(ω) and imaginary part jσ``(ω).

$$\sigma(\omega) = \sigma`(\omega) + j\sigma``(\omega) \qquad (4)$$

$$\sigma`(\omega) = \sigma_{dc} + A\omega^n \qquad (5)\ [4,5,14,20,6,24,7,10,8,16]$$

where σ_{dc} is the dc conductivity, A is a constant with conductivity unit, and n is the power law exponent, takes the value between 0 and 1.

Alternative representations of the experimental data are the complex permittivity, and the relation between the complex conductance and complex impedance are given in equation as.

$$Y = \omega c - \frac{1}{\omega L}$$
$$Z = \omega L - \frac{1}{\omega c} \qquad (6)$$

Recent examination of the scaling properties of σ (ω) and ε(ω) have shown complementary diagram for each other, as in Figures(1) to (9).

The corresponding form of the equation(6) for the dielectric permittivity is

$$Tan\delta = \frac{\varepsilon``(\omega)}{\varepsilon`(\omega)} = \frac{\sigma`(\omega)}{\sigma``(\omega)} \qquad (7)$$

Cole-Cole plot of ε" and ε' gives useful information for the relaxation processes that occur in the specimens. It can be seen that, at each temperature, it is displayed as a semicircular arc. The arc representation is:

$$\sin^2(\delta) = \left(\frac{\varepsilon``}{\sqrt{\varepsilon`^2 + \varepsilon``^2}}\right)^2$$

The complement of the arc is represented as:

$$\cos^2(\delta) = \left(\frac{\varepsilon`}{\sqrt{\varepsilon`^2 + \varepsilon``^2}}\right)^2$$

$0 \leq \delta \leq 90$

The relation between the complex dielectric and complex conductivity is diagramed as function of frequencies.

Figs (17) to (25), represent the contribution between the real parts and the imaginary parts of the dielectric and conductivity, and is given as:

σ`` ε`` = σ` ε` ,

$\frac{\sigma`}{\varepsilon``}$ is the real part and $\frac{\sigma``}{\varepsilon`}$ is the imaginary part

The equations represent the conduction with temperature and frequency for each sample is given as:

$$\sigma \propto f \quad , \quad \varepsilon \propto \frac{1}{f} \ and \ \sigma = \varepsilon f$$

The range of temperature is taken between 273K +room to 573K, and the frequency range is taken between 170Hz and 100KHz.

The conductance in this samples as a result of displacement of two kinds of charge carriers is in opposite directions and other charge carriers hoping between in. The equation representing this mechanism is given as.

$$\frac{\sigma'^2}{\varepsilon''^2} + \frac{\sigma''^2}{\varepsilon'^2} = 4f^2$$

The conducting between those two types(intermediate temperature), when the two parts of conductivity and dielectric are equaled and in this case , there is a resonance and the conductance as a result of displacement is equal to the conductance as a result of hoping.

By taking any figure with intersect between the real and imaginary conductivity or dielectric, the major conductance below this tangent point between the real and imaginary is a result of displacement; and the major conductance, above the tangent point, is a result of hoping.

The maximum value of tanδ confirms the important contribution of the conductivity to the dielectric permittivity in these samples. The peaks in the tanδ verses Log$f$ plots are observed, corresponding to dielectric relaxation phenomena. The maximum of tanδ is observed at a frequency f_{max} specific for each temperature. To obtain the relaxation time $\tau_{tan\delta}$ for each sample at a certain peak and temperature, from the condition.

$$\tau_{tan\delta}\ f_{max} = 1 \qquad (8)$$

To find the activation energy of the samples, from An Arrhenius plot of Log $\tau_{tan\delta}$ versus 1/T, then an activation energy is given in Table(3).

Table (3). The value of the activation energy as E/K with Ni-ion content

X (Nickel content)	Slope (E/K) activation energy per Boltzmann's constant	Slope (E/K) activation energy per Boltzmann's constant(samples doped by Yttrium)
1	0.459	1.984
0.5	0.7067	-0.2487
0	1.011 (at room temperature)	0.1776

Fig(26) represents the grain sizes with the composition of Al-Ni ferrite and Al-Ni ferrite with yttrium showing the effect of yttrium and making the grain size smaller (x=0.0, Y) and the conductivity of the sample low at room temperature. To compare between the Fig(1) and Fig(4), this means the grain size of the sample with yttrium nearly becomes large with high temperature and the conductivity of the sample also increases.

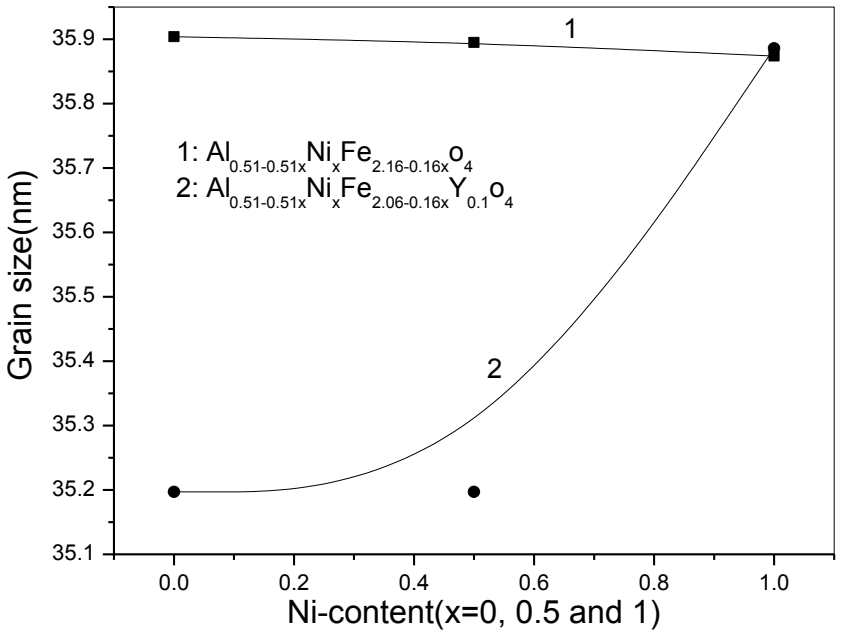

Fig(26).The variation of grain size of all samples as a function of Ni- content (composition x=0, 0.5 and 1) .

Fig. (27) represents the activation energy with composition of Al-Ni ferrite and Al-Ni ferrite with yttrium The activation energy,(E/K) k (K is the Boltzmann constant and k is the international unit of temperature), which is given from the relaxation time of each sample at different temperature. The activation energy is increased from the sample with x=1, Ni Fe_2 O_4 to the sample with x=0.0, $Al_{0.51}$ Fe_2 O_4 as shown in the figures. The samples doped by Yttrium show the behavior of activation energy, which decrease from the sample with x=0 to reach the sample with x=0.5 after that, the activation energy increased in the sample with x=1 .

The activation energy behavior of the samples with Ni-content looks like the grain size represented in Fig(26,27).

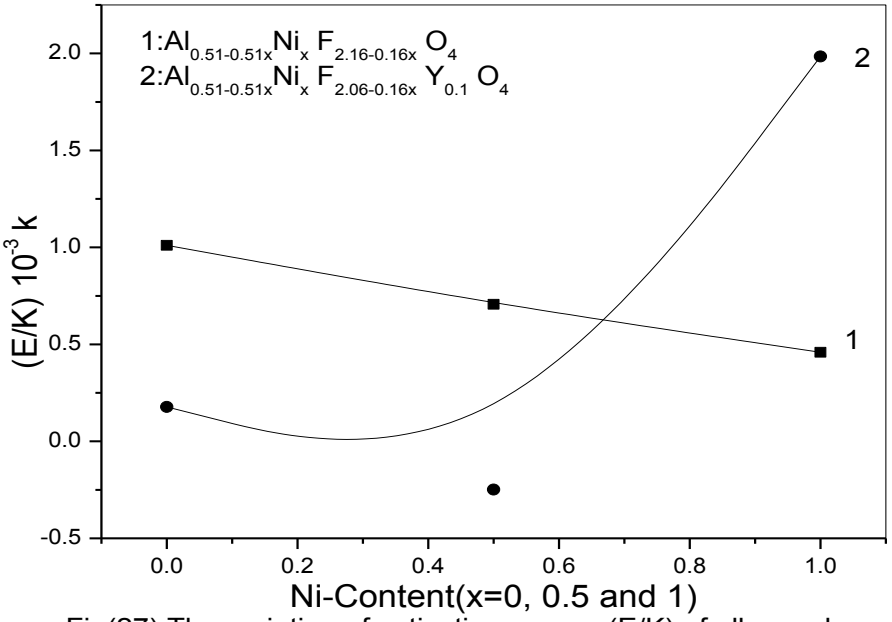

Fig(27).The variation of activation energy (E/K) of all samples as a function of Ni- content (composition x=0, 0.5 and 1) .

Conclusion

The X-ray diffraction analysis of the samples ensures the formation of S-type spinal ferrite without any residuals of the original constituent oxides. Ac conductivity, dielectric constant are investigated by using the complex impedance technique, (at and above room temperature). The conductance results specify two types of conduction mechanisms, Cole-Cole diagrams show the existence of a distribution of relaxation times and give values of the activation energy of the dielectric relaxation process. The average particle size estimated is 35.1-35.9nm.

Acknowledgements

I would like to express my deepest gratitude and thanks to Prof. Dr. M.K. Elnimr, Prof. Dr. A.m. Abo Elata, Prof. Dr. S.A Saafan, Prof. Dr. D.Elkony.

The samples were prepared, and all measurements were taken in the Lab. of Material Science and Electronic LAB.

Lab. Material Science and Electronic
Physics Department
Tanta University

References

1. Ahmed A., (1992) "Investigation of structural transport and magnetic properties of the system Li0.25Cu0.5Fe2.25-xAlxO4"., J. Mater. Sci., 27,15, 4120-4124.
2. Ahmed M.A., Mansor S.F., Afifi M., (2012) "Structural and electrical properties of Nano metric Ni-Cu ferrites synthesized by citrate precursor method"., J. Magn. Magn. Mater. 324,1, 4-10.
3. Aslibeiki B., (20014) "Nanostructure, magnetic and electrical properties of Ag doped Mn-ferrite nanoparticles"., Current Appl. Phys. 14,12, 1659-1664.
4. Al-Hammadi A.H. (2010) "Complex dielectric constant and complex conductivity of Al-Ni ferrous metals"., University of Aden Journal of Natural and Applied Sciences., 14, 3, 675-696.
5. Abo Elata A.M., Elnimr M.K, Attia S.M., Elkony D. and Al-Hammadi A.H., (2006) "Studies of AC electrical conductivity and initial magnetic permeability of rare-earth substituted Li-Co ferrites"., J. Mag. Mag. Mater., 297,1, 33-43.
6. Abo Elata A.M., Elnimr M.K, Elkony D. and Al-Hammadi A.H., (1999) "Conduction mechanism of BaCo2-xNixFe16O27"., J. Mag. Mag. Mater., 202,2-3, 397-404.
7. Abo Elata A.M., Elnimr M.K, Elkony D. and Al-Hammadi A.H(1999)., Dielectric and magnetic permeability behavior of BaCo2-xNixFe16O27 W-type hexa-ferrites., J. Mag. Mag. Mater., 204,1-2, 36-44.
8. Abo Elata A.M., Elnimr M.K, Attia S.M., Elkony D. and Al-Hammadi A.H., (2005) "Spectral, initial magnetic permeability and transport studies of Li0.5-0.5xCoxFe2.5-0.5xO4 spinel ferrites"., J. Mag. Mag. Mater., 295,1, 28-36.
9. Balachandron Ruthramurthy, Ce-Yi Ho, Koay Yen Wei, Yow Ho Kwang, Tan Kar Bon, Ahmod Fauzi Mohd Noor, (2010) "Synthesis of Ba0.6Sr0.4TiO3 Nano powder through slow rate sol-gel route as a dielectric material"., World Appl. Sci. J. 9,9, 29-33.
10. Elliott S.R (1987)., AC conduction in amorphous chalcogenide and pnictide semiconductors., "Advances in physics" 36,2, 135-217.
11. Goldman A.,(1993) "Modern ferrite technology", Mareel Dekker, Ine. New York,
12. Galasso F.S., (1969) "Structure, properties and preparation of proves kite- type".
13. Hassan A.K., and Gou R.D., (1992) "Structure studies of thermally evaporated thin films of Cu-phthalocyanine"., Phys. Stat. Sol. (a) 132,1, 91-101.
14. Iwauchi K., Ikeda Y., (1986) "Dielectric properties of hexagonal ferrites"., Phys. Stat Sol. (a) 93,1, 309-313.
15. JCPDS – ICDD (c) (1991).
16. Jonscher A.K., (1983) "Dielectric relaxation in solid", Chelsea Dielectrics Press, London,
17. Kuanr B.K. and Srivastava G.P.,(1994) "Dispersion observed in electrical properties of titanium substituted lithium ferrites"., J. Appl. Phys., 75, 6115.
18. Koops C.G., (1951) "Dispersion of resistivity and dielectric constant of some semiconductors at audio frequencies"., Phys. Rev. , 83, 121.
19. Liu C.S., Shu W.B., Tung M.J. and Ke M.Y., (1990) "Effect of partial substitution of Ge^{4+} for Zn^{2+} on the microstructure and temperature stability of Mn-Zn ferrites"., J. Appl. Phys. 67, 5506.
20. Long A.R., (1982) "Frequency–dependent loss in amorphous semiconductors"., "Advances in Physics" 31,5, 553-637.
21. Mazen S.A., Abdel-Daiem A.M.,(2011) "IR spectra and dielectric properties of Cu-Ge ferrites"., Mater. Chem. and Phys. 130,3, 847-852.
22. Mazen S.A., (1996) "The conduction mechanism of Li-Ge ferrites"., Phys. Stat.Sol. 154,9, 681-691.
23. Macdonald J.R., (1987) "Impedance Spectroscopy"., New York, Jon Wily and Sons.
24. Mondal R.A., Murty B.S., Murthy V.R.K. (2014) "Maxwell-Wagner polarization in grain boundary segregate NiCuZn ferrites"., Current Appl. Phys. 14,12, 1727-1733.
25. Reddy P.V.,Rao S.M.D. and Rao T.S., (1981) "Electrical conductivity of Li-Ni ferrites"., J. Less. Comm. Meta. 79,2, 191-198.
26. Toolonaar F.J.C.M. and Vanlierop Verhees M.T.J., (1989) "Reactive sintering of Mn-ferrites"., J. Mater. Sci, 24,2, 402-408.

دراسة الخصائص التركيبية والكهربية لمركبات النيكل والألمونيوم فرايت مطعمة بالديتريوم

عبد الحكيم احمد عبد الجليل الحمادي
قسم الفيزياء، كلية العلوم جامعة صنعاء، صنعاء اليمن
DOI: https://doi.org/10.47372/uajnas.2015.n1.a18

الملخص

تم تحضير مجموعة من العينات المحضرة لبعض مركبات النيكل ألمونيوم المطعمة بالد يتريوم ذو الصيغة الكيميائية.
$Al_{0.51-0.51x}Ni_xFe_{2.16-0.16x}O_4$ and $Al_{0.51-0.51x}Ni_xFe_{2.06-0.16x}Y_{0.1}O_4$ where (x = 0.0, 0.5, and 1)
تم تحضير العينات بالطريقة السيراميكية, ثم تم التلبيد مرتين عند درجات حرارة مختلفة. تم التحقق من أنَ العينات مكعبة التركيب البلوري من النوع S (spinel ferrites) وذلك باستخدام حيود الأشعة السينية تمت دراسة الموصلية الكهربية للتيار المتردد, ثابت العزل الكهربي والفقد في العزل لهذه العينات باستخدام تكنيك المعاوقة المركبة. تمت قياسات العينات المنوط بالاختبار عند درجة حرارة الغرفة ودرجات مختلفة فوق حرارة الغرفة وكذلك عند ترددات مختلفة. أظهر وجود توزيع احتمالي لأزمنة الاسترخاء وأعطى قيما لطاقة التنشيط الخاصة بعملية استرخاء ثابت العزل. ظهور تماثل بين حجم البلورة وطاقة التنشيط في العينات.

الكلمات المفتاحية: اكاسيد المونيوم- نيكل- حديد و د يتريوم, البلورة بالنانو, الموصلية الكهربية وخصائص العزل الكهربي.